Symmetry, density of doping holes, and T_c in superconducting thallium cuprates

N. Merrien, L. Coudrier, C. Martin, A. Maignan, and F. Studer
Laboratoire de Cristallographie et Sciences des Matériaux, Institut des Sciences de la Matière et du Rayonnement, boulevard du Maréchal Juin, 14050 Caen Cedex, France

A. M. Flank
Laboratoire pour l'Utilisation du Rayonnement Electromagnétique, Bâtiment 209d, 91405 Orsay Cedex, France
(Received 18 October 1993)

Polarized Cu L_3 absorption experiments have been made on $Tl_2Ba_2CaCu_2O_{8\pm\delta}$ well-oriented thin films by x-ray spectroscopy. Using a fitting procedure, the doping hole density per copper atom has been measured to be 16%. The results are in agreement with a doping occurring only with the (x,y) symmetry in the $[CuO_2]_\infty$ planes of these layered structures. Unpolarized XAS experiments have also been conducted on Tl(2:2:0:1), Tl(2:2:1:2), Tl(2:2:2:3), and Tl(1:2:2:3) ceramics with different doping and superconducting properties. The results show that, in the copper monolayer compound, the change in the doping hole density is accompanied by a drastic change of T_c while this effect appears less important in the copper bilayer compounds and even uneffective in the three-layer one. These results show that the doping hole density is a key factor to monitor the superconducting properties and that the number of copper layers also plays an important role.

I. INTRODUCTION

As is now well known,[1,2] the cuprate superconductors have two types of holes: the covalent holes as in CuO, Nd_2CuO_4, and La_2CuO_4, etc. and the doping holes. The former are created as a result of charge transfer from ligand (oxygen) to metal (copper) giving rise to a Cu $3d^{10}\underline{L}$ configuration in the ground state in addition to the Cu $3d^9$ configuration. The superconducting cuprates as also the formally trivalent cuprates such as $NaCuO_2$ or $La_2Li_{0.5}Cu_{0.5}O_4$ are characterized by the presence of doping holes created as a result of either cation doping as in $La_{1-x}Sr_xCuO_4$, excess oxygen as in $YBa_2Cu_3O_{6+\delta}$, and/or electron transfer as in the bismuth- and thallium-layered superconductors. It is these doping holes rather than the localized covalent holes that get paired to yield superconductivity and are characterized by a $3d^9\underline{L}$ configuration, having a binding energy higher than either $3d^9$ or $3d^{10}\underline{L}$ in the ground state of the system.

The high-energy spectroscopies have from the very beginning played a key role in study of the electronic configuration of high-T_c superconductors. Core-level photoemission from Cu $2p$, O $1s$, and other cations (e.g., Ba $4d$, Ba $3d$, Bi $4f$, Bi $5p$, Sr $3d$),[1-5] valence-band photoemission,[6,7] Cu K-edge x-ray absorption;[8-11] Cu L_3-edge,[1,2,12-14] O K-edge x-ray absorption,[14-16] resonant photoemission spectroscopy;[17,18] Auger emission spectroscopy,[19] and, more recently, the angle-resolved ultraviolet photoemission and inverse photoemission spectroscopies[20-22] have been gainfully employed in study of these systems.

Cu L_3-edge x-ray absorption has yielded a wealth of information about the absence or presence of an additional shoulder on the high-energy side, ascribed to the dipole transition $2p^63d^9\underline{L}\rightarrow 2p^53d^{10}\underline{L}$, in order to determine the status of the system with regard to the question of doping holes and even to provide a quantitative measure for the same.[13,23] The main absorption line itself is ascribed to the dipole transition $2p^63d^9+2p^63d^{10}\underline{L}\rightarrow 2p^53d^{10}$.

Measurements of doping hole concentration in this way provide a way to study the question of an optimum value of hole concentration in terms of critical temperature in these systems. As is now well known, the T_c in these systems, amongst other things, depends highly on the concentration of the doping holes and tends to decrease when the hole density departs from a certain optimum value for the system. It has been shown that, for instance, in the $TlBa_2Ca_{1-x}Nd_xO_{7-\delta}$ series ($0.2\le x\le 1$) (Ref. 13) or in the $Bi_{2-x}Pb_xSr_2Ca_{1-x}Y_xCu_2O_{8-\delta}$ ($0\le x\le 1$),[23] the decrease of T_c's with increasing x corresponds to a similar decay of the $2p^63d^9\underline{L}\rightarrow 2p^53d^{10}\underline{L}$ transition and of the doping hole density.

On Bi (2:2:1:2) crystals and thin films, the polarized x-ray absorption spectroscopy (XAS) results, reported so far, seem to agree with the conclusion that Cu $3d$ covalent holes are of $d_{x^2y^2}$ symmetry with a 10–20% admixture of Cu $3d_{z^2-r^2}$ holes[24-28] whereas the doping holes exhibit only the (x,y) symmetry, i.e., are present only in the $[CuO_2]_\infty$ planes. The presence of doping holes along the z axis has been detected in $La_{2-x}Sr_xCuO_4$ by some authors[50] and still remain an open question. Conversely the symmetries of covalent and doping holes in the thallium cuprates is far from being understood as well as in bismuth cuprates; this lack of polarized XAS results may be due, till recently, to the preparation difficulties of superconducting thallium cuprates crystals and thin films of good quality.

One of the few papers reporting about polarized XAS of thallium cuprates is due to Romberg *et al.*[29] in which the Cu L_3 and O K edges have been recorded on a Tl(2:2:1:2) single crystal using high-energy electron-energy-loss spectroscopy (EELS). The main result of this study is the observation of an intense prepeak at 529 eV

on the O K-edge spectrum for the incident electric vector **E** parallel to the **c** axis. According to calculations of photoemission, inverse photoemission, and x-ray emission spectra, the prepeak has been ascribed to oxygen atoms in the $[BaO]_\infty$ layers, i.e., to the apical oxygens of the CuO_5 pyramids. This result suggests that a high density of holes must be found in the O $2p_z$ orbital of the copper apical oxygen. It should correspond to a large shoulder around 933 eV on the Cu L_3-edge spectrum, recorded with $\mathbf{E}\|c$, due to the $2p^6 3d^9 \underline{L} \rightarrow 2p^5 3d^{10} \underline{L}$ transition along the z direction. Conversely only a small peak around 934 eV has been observed by EELS on the $\mathbf{E}\|\mathbf{c}$ Cu L_3 edge, which has been suggested by Romberg *et al.* to belong to some amount of a monovalent copper compound although no impurity phase was detected by x-ray diffraction. Dealing with polarized XAS in single crystals of Tl(2:2:1:2) and Tl(2:2:2:3), the same group[39] has recently confirmed these results and shown that the doping hole density per copper stands around 0.17 in both compounds for T_c's which are not the optimized ones, 113 and 118 K, respectively.

In order to understand the covalent and doping-hole symmetries in thallium cuprates, we have investigated the polarized Cu L_3 edge of a well characterized thin film of $Tl_2Ba_2CaCu_2O_8$. In the same time, the density of doping holes in the $[CuO_2]_\infty$ planes of most of the known superconducting thallium cuprates (2:2:0:1, 2:2:1:2, 2:2:2:3, and 1:2:2:3) will be deduced from the Cu L_3 edges recorded on ceramics and compared to the corresponding T_c's. In a second time, the copper L_3 edges of Tl(2:2:0:1) and Tl(2:2:1:2) phases, annealed in H_2/Ar, have been recorded in order to evidence any variation of the doping hole density with annealing time and to correlate them with the T_c's increase.

II. EXPERIMENT

The $Tl_2Ba_2Ca_1Cu_2O_{8+\delta}$ thin films have been synthesized by *ex situ* annealing of a stoichiometric material deposited by cathodic sputtering on a $LaAlO_3$ (100) substrate. The sputtering module consists of four targets corresponding to the different elements present in the desired phases of the Tl-Ba-Ca-Cu oxides family facing a rotating substrate holder. The sputtering is realized in an atmosphere composed of oxygen and argon in the 1:10 ratio. The total pressure of 2.2×10^{-2} mbar enables the sputtering in both the dc and rf modes which are necessary due to the various target natures, metallic for thallium and copper and insulating for barium and calcium. Indeed both the latter targets are oxides and can only be sputtered in a rf mode at 13.56 MHz. The desired stoichiometry is obtained by varying the voltages applied to the four different targets electrically independent. The substrate holder rotating at a rate of 10 rpm is the common anode and the thin film is obtained by facing sequentially the different targets.

Post annealing necessary to crystallize the selected phase is realized in a sealed quartz tube which limits the pollution by thallium. The high volatility of this element and of its oxides hinders the *in situ* synthesis from sputtering. After sputtering, thin films are then wrapped in a gold foil in the presence of a Tl(2:2:1:2) pellet in order to introduce a thallium oxide pressure, and sealed in a quartz tube which is evacuated down to 2×10^{-2} mbar. The annealing cycle consists in a fast heating at 10 °C/min before a dwell around 850 °C during 10 min and a cooling down at 3 °C/min. The obtained crystallized thin films are monophasic, $Tl_2Ba_2Ca_1Cu_2O_{8+\delta}$, as seen by x-ray diffraction and exhibit homogeneous platelets with the **c** axis perpendicular to the substrate plane. The film thickness has been measured by a Dectac profilemeter after wet chemical etching and has been found to be about 1 μm. Then magnetic susceptibility study indicates a transition at 105 K and the x-ray spectrum exhibits the 001 reflections only. The analysis of the thin film used in XAS, performed with a scanning electron microscope equipped with a Tracor energy dispersive spectroscope, leads to the composition $Tl_{2.2}Ba_{1.6}Ca_{1.2}Cu_2O_x$ fairly close to the theoretical formula.

For the ceramics synthesis, the oxides Tl_2O_3, BaO_2, CuO, and Nd_2O_3 were mixed in the adequate ratios. The mixtures were pressed into rods of 4 mm diam $\times$ 50 mm lengths (about 2 g weight) and heated in evacuated quartz ampoules (heating rate: 150 °C/hr, reaction time: 24 h at 950 °C, cooling rate: 8 °C/h from 950 to 600 °C and then furnace cooled). The lanthanum cuprate La_2CuO_4 [reference compounds for Cu(II) formal valence state], was prepared from the oxides La_2O_3 and CuO, mixed and heated in air in platinum crucibles at 1100 °C.

The Cu(III) reference oxide $La_2Cu_{0.5}Li_{0.5}O_{4-\delta}$ was synthesized from a mixture of the oxides La_2O_3, CuO, and of lithium carbonate Li_2CO_3.[30] The preparation was pelletized, heated in flowing oxygen at 900 °C for 12 h and cooled to room temperature at the rate of 50 °C/h. Thermogravimetric analysis (TGA) could not be performed on this sample due to the possibility of lithium loss during the reduction. Iodometric titration confirmed the presence of trivalent copper and led to a δ value close to 0.04.

These materials were checked by x-ray and electron diffraction for purity and defects density. Superconducting properties were studied by susceptibility measurements. Structure determinations and physical properties of these compounds have been published elsewhere.[31–37]

All the XAS spectra at the L_3 edge of copper were recorded at room temperature. The experiments were performed at LURE (Orsay) using the synchrotron radiation from the super-ACO ring operated at 800 MeV with a typical current of 250 mA. Samples were ground and sieved homogeneously on a sticky band supported by an aluminum sample holder. Electrical contacts were realized by silver paste dots. The x rays were monochromatized by two beryl crystals ($10\underline{1}0$) and the absorption coefficient measured in total yield mode (TEY) using either a detection of the electrons by a channeltron or the measure of the sample current. The energy scale was then positioned with respect to the $|3d^9\rangle$ peak of CuO at 931.2 eV. The experimental energy resolution was estimated to be better than 0.3 eV, whereas the reproducibility of the energy position of the spectra features is close to 0.05 eV. The width of the core hole has been

measured to be 0.56 eV at the L_3 edge.[38] The usual thickness of the probed upper layer of the samples is about 200 Å in the total electron yield method.

Dealing with soft x-ray spectroscopies on ceramics, one of the main problems concerns the effect of the grain boundaries on the spectra, since the TEY detection mode is more sensitive to surface effects than the fluorescence yield (FY) mode. Trying to be as close as possible to the bulk information, we systematically have ground the sintered ceramics immediately before spreading the powder on an adhesive tape; the sample holder was immediately placed in the high vacuum chamber. This allows grains to be broken, fresh surfaces to be revealed, and prevents the formation of carbonates on the surface. Of course, this process will not prevent the formation of oxygen layers on the surfaces but these are of small influence at the copper L_3 edge.

The normalization has been made on the continuum before the L_2 peak around 940 eV. But, in order to compare directly to $|3d^9\underline{L}\rangle$ peak intensity on some figures, the top of the $|3d^9\rangle$ transitions has been set to a common value chosen arbitrarily. To obtain the relative intensities of the transitions, the spectra have been least-squares fitted by a combination of Gaussian and Lorentzian shapes using a program written by Rodriguez to fit neutron-diffraction line profiles. The initial program has been modified to take into account the specificities of x-ray absorption data and to introduce a linewidth per peak as a fitted parameter.

III. RESULTS AND DISCUSSION

A. Reference compounds

1. Structure

In nonsuperconducting La_2CuO_4, the octahedral coordination of copper (II) is the result of an intergrowth between single rocksalt $[LaO]_\infty$ layers and single perovskite $[LaCuO_3]_\infty$ layers; nevertheless due to the Jahn-Teller effect a strong distortion of the CuO_6 octahedra occurs which stabilizes long Cu-O distances along the c axis ($2\times d_{\text{Cu-O}}\approx 2.40$ Å) and short distances in the basal planes ($4\times d_{\text{Cu-O}}\approx 1.98$ Å).

The reference for Cu(III) species, $La_2Li_{0.5}Cu_{0.5}O_{4-\delta}$, is a K_2NiF_4-type oxide synthesized under high pressure.[37] In this phase, Cu and Li cations are distributed into distorted octahedral sites. The chemical analysis of the latter oxide showed in fact a mixed valency of copper with 85% of Cu(III) and 15% of Cu(II) suggesting oxygen deficiency.

2. Copper L_3 edge

Copper L_3-edge spectra of cuprates La_2CuO_4 and $La_2Li_{0.5}Cu_{0.5}O_{3.96}$ taken as references for Cu(II) and Cu(III) valence states, respectively, are shown in Fig. 1 together with the fitted curves.

The spectrum of the first compound is characterized by one peak centered around 931.2 eV and 0.53 eV half width at half maximum (HWHM): The results

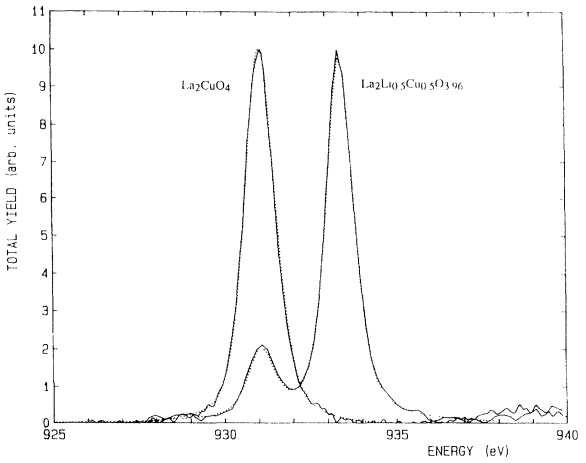

FIG. 1. Copper L_3 edge of the La_2CuO_4 and $La_2Li_{0.5}Cu_{0.5}O_{3.96}$ reference compounds for the Cu(II) and the Cu(III). The two peaks at 931.1 eV and 933.45 eV are associated with $|2p_{3/2}3d^9\rangle+|2p_{3/2}3d^{10}\underline{L}\rangle\rightarrow|\underline{2p}3d^{10}\rangle$ (covalent holes) and $|2p_{3/2}3d^9\underline{L}\rangle\rightarrow|\underline{2p}3d^{10}\underline{L}\rangle$ (doping holes) transitions, respectively.

of the simulation are presented in Table I. This single peak corresponds to the transition $|2p_{3/2}3d^9\rangle\rightarrow|\underline{2p}3d^{10}\rangle$, giving rise to the copper final state $[1s^{\overline{2}}2s^{\overline{2}}2p^53s^23p^63d^{10}4s^04p^0]$.

The spectrum of $La_2Li_{0.5}Cu_{0.5}O_{3.96}$ exhibits two peaks, clearly visible due to their large energy difference: The intensity of the second peak at $E_1=933.45$ eV (Table I) is quite larger than the other one at $E_0=931.1$ which keeps the same HWHM. The energy of the first peak is close to the values found for the Cu(II) reference La_2CuO_4 and thus corresponds to the same transition $|2p_{3/2}3d^9\rangle\rightarrow|\underline{2p}3d^{10}\rangle$, attesting for the presence of Cu(II) valence state in small amount. The second peak, as shown in previous papers,[12] is due to the $|2p_{3/2}3d^9\underline{L}\rangle\rightarrow|\underline{2p}3d^{10}\underline{L}\rangle$ transitions.

From the intensities of both peak $I_{|3d^9\rangle}$ and $I_{|3d^9\underline{L}\rangle}$, one can deduce a mean density of hole per copper $n_h=I_{|3d^9\underline{L}\rangle}/(I_{|3d^9\rangle}+I_{|3d^9\underline{L}\rangle})=0.85$ in good agreement with the chemical analysis. It is worth noting here that, in the charge-transfer model, the hole density in the $2p_{x,y}$ oxygen band should only be 0.425 due to the small copper concentration in this cuprate.

TABLE I. Simulation parameters of the copper L_3 edges of the nonreference compounds. E and Γ are, respectively, the energy and the HWHM of the lines in eV. $n_h=I_{|3d^9\underline{L}\rangle}/(I_{|3d^9\underline{L}\rangle}+I_{|3d^9\rangle})$ is the density of hole per copper.

Compounds		$\lvert 3d^9\rangle$ $2p_{3/2}\rightarrow 3d^9$	$\lvert 3d^9\underline{L}\rangle$ $2p_{3/2}\rightarrow 3d^9\underline{L}$	n_h (±0.015)
La_2CuO_4	E	931.2		
	Γ	0.53		
$La_2Li_{0.5}Cu_{0.5}O_{3.96}$	E	931.1	933.45	
	Γ	0.46	0.47	0.84

B. The Tl(2:2:1:2) thin film

The Cu L_3-edge spectra of a Tl(2:2:1:2) thin film have been recorded at room temperature in TEY mode for five orientations of the incident electric field with respect to the film surface, i.e., to the (a,b) plane of the structure (Fig. 2). The normalization has been realized above 937 eV on the continuum in order to get the relative intensities of the $|3d^9\rangle$ and $|3d^9\underline{L}\rangle$ peaks for the various orientations.

Like in single crystals and thin films of Bi(2:2:1:2), the intensity of the $|3d^9\rangle$ peak ($|2p_{3/2}3d^9\rangle \rightarrow |\underline{c}2p_{3/2}3d^{10}\rangle$ transition) decreases when increasing the angle Θ of the incident electric field with respect to the film surface [Fig. 3(a)] till a 14% intensity for the ratio $I_{|3d^9\rangle(\Theta)}/I_{|3d^9\rangle(0°)}$ at $\Theta=75°$. Using a dipolar angular variation of the form $I_{|3d^9\rangle(0°)}\cdot\cos^2(\Theta)+I_{|3d^9\rangle(90°)}\cdot\sin^2(\Theta)$, the intensity along the z axis $I_{|3d^9_{z^2}\rangle}$ can be extrapolated at $\Theta=90°$ [Fig. 3(a)] and the density of covalent holes per copper n_z, estimated through the formula $n_z=I_{|3d^9_{z^2}\rangle}/(I_{|3d^9_{x^2-y^2}\rangle}+I_{|3d^9_{z^2}\rangle})$, is found to be 0.11. This result is in good agreement with recent results obtained by XAS at the Cu L_3 edge using the FY mode in Tl(2:2:1:2) and Tl(2:2:2:3) single crystals by Pellegrin *et al.*[39]

The intensity of the $|3d^9\underline{L}\rangle$ peak ($|2p_{3/2}3d^9\underline{L}\rangle \rightarrow |\underline{c}2p_{3/2}3d^{10}\underline{L}\rangle$ transition) decreases when increasing the angle Θ of the incident electric field with respect to the film surface [Fig. 3(b)] till a 10% intensity for the ratio $I_{|3d^9\underline{L}\rangle(\Theta)}/I_{|3d^9\underline{L}\rangle(0°)}$ at $\Theta=75°$. An example of simulation with two Lorentzian contributions is shown in Fig. 4 and the least-square fitting parameters are given in Table II for all five orientations. Between 0° and 35°, no significant change of the $|3d^9\underline{L}\rangle$ peak relative intensity has been recorded (Table II) probably due to some kind of c-axis distribution of the crystallites around the normal

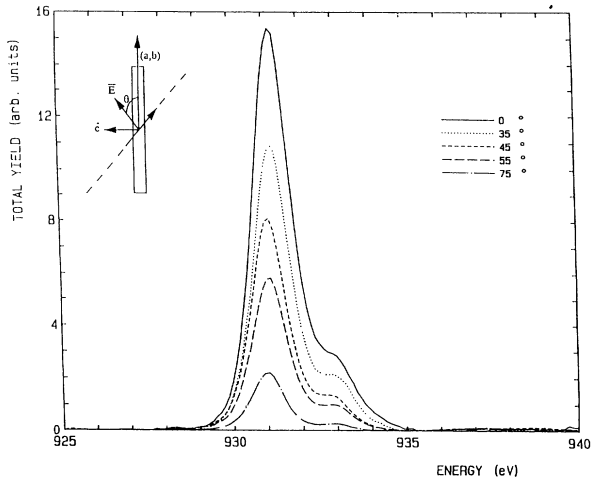

FIG. 2. Cu L_3-edge spectra of the Tl(2:2:1:2) thin film measured with **E** at 0° (——), 35° (· · · ·), 45° (- - -), 55° (— — —), and 75° (—·—·—·) to the (a,b) plane. The spectra are normalized at a point far away from the peak (above 937 eV) to highlight the large variations in the intensity of the Cu L_3 ($2p \rightarrow 3d$) peak with orientation.

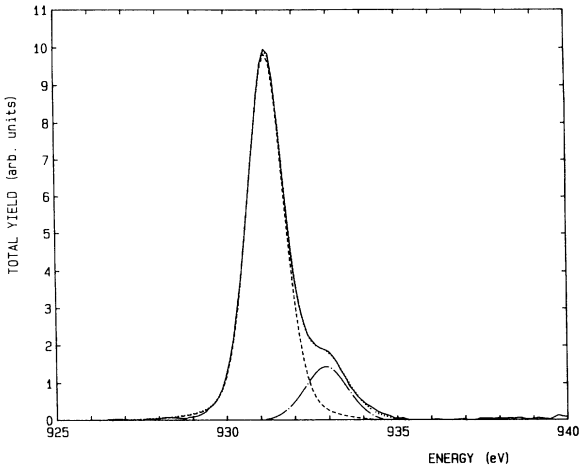

FIG. 3. Simulation curves at copper L_3 edge for the polarized spectrum with $\mathbf{E}\|(a,b)$. The two Gaussians represent the relative intensities of the Cu $3d^9$ and Cu $3d^9\underline{L}$ states: (——) experimental, (· · · ·) total fit, (- - -) $|3d^9\rangle$, and (—·—·—·) $|3d^9\underline{L}\rangle$.

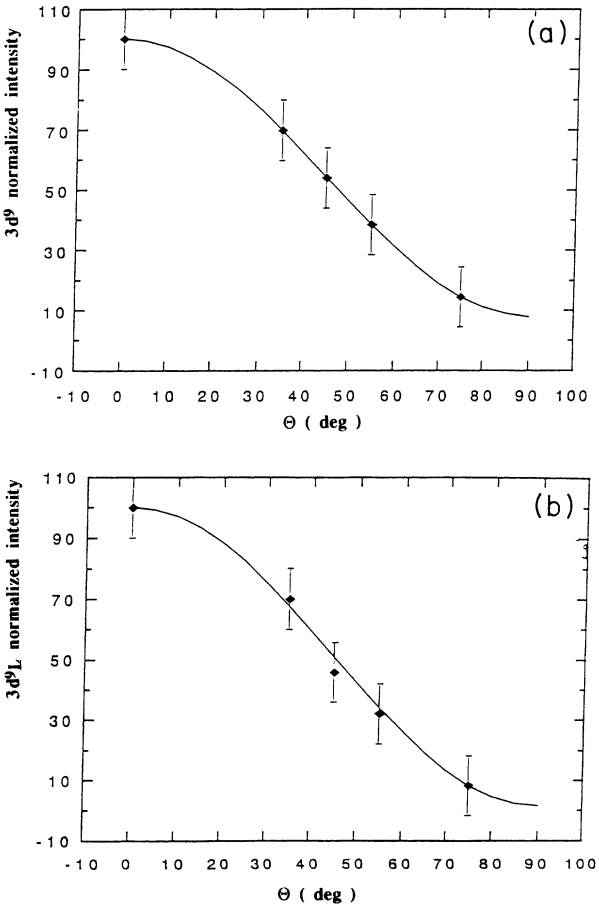

FIG. 4. Variations of the total $3d^9$ (a) and $3d^9\underline{L}$ (b) normalized intensities versus the angle θ between the incident electrical field and the (a,b) plane of the Tl(2:2:1:2) structure. A fit by a law of the type $I(\theta)=I_{0°}\cos^2(\theta)+I_{90°}\sin^2(\theta)$ allows an extrapolation to 90° to be performed.

TABLE II. Simulation parameters of the copper L_3 edge for five orientations of the incident electric field with respect to the (a,b) plane of the Tl(2:2:1:2) thin film ($T_c = 105$ K). θ is the angle between electric field **E** and (a,b) plane and E and Γ are, respectively, the energy and the HWHM of the lines in eV.

Orientation		$\|3d^9\rangle$ $2p_{3/2} \rightarrow 3d^9$	$\|3d^9\underline{L}\rangle$ $2p_{3/2} \rightarrow 3d^9\underline{L}$	$I_{\|3d^9\underline{L}\rangle(\theta)}/(I_{\|3d^9\underline{L}\rangle(\theta)}+I_{\|3d^9\rangle(\theta)})$
	E	931.2	932.91	
$\theta=0°$	Γ	0.63	0.77	0.16
	E	931.17	932.92	
$\theta=35°$	Γ	0.62	0.68	0.16
	E	931.16	932.91	
$\theta=45°$	Γ	0.60	0.68	0.135
	E	931.07	932.91	
$\theta=55°$	Γ	0.60	0.65	0.13
	E	930.98	932.92	
$\theta=75°$	Γ	0.55	0.56	0.09

to the thin-film surface and also to the precision of the goniometer mounted on the experiment. The extrapolation of these intensities to $\Theta=90°$ [Fig. 3(b)] shows that the $|3d^9\underline{L}\rangle$ peak vanishes for the incident electric field parallel to the **c** axis. This result shows that the doping holes seem to be present only in the $[CuO_2]_\infty$ planes of the Tl(2:2:1:2) compound like in Bi(2:2:1:2) and Tl(2:2:1:2) thin films and single crystals, at least within the experimental errors which stand around a few percent of the white line intensity. The density of doping holes per copper n_h, estimated through the formula $n_h = I_{|3d^9\underline{L}\rangle}/(I_{|3d^9\rangle}+I_{|3d^9\underline{L}\rangle})$, is found to be 0.16 for $T_c = 105$ K to be compared to $n_h = 0.17$ found by Pellegrin *et al.*[39] on a Tl(2:2:1:2) single crystal ($T_c = 113$ K).

In Fig. 5, the Cu L_3 edge corresponding to three orientations are normalized on the $|3d^9\rangle$ peak in order to show first, the decrease of the $|3d^9\underline{L}\rangle$ peak as a function of the angle between the incident electric field and the thin-film plane, and second, to evidence the energy shift

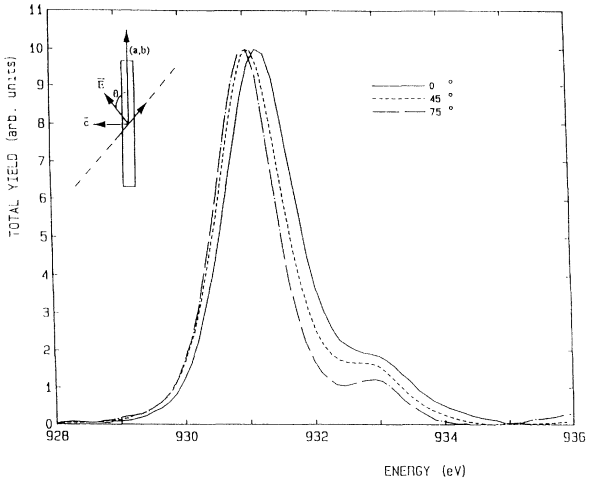

FIG. 5. Cu L_3-edge XAS spectra of the Tl(2:2:1:2) thin film measured with **E** at 0° (——), 45° (- - -), and 75° (—·—·—·) to the (a,b) plane. The spectra are normalized to their peak positions for better appreciation of the systematic shift of the peak to lower energy with increasing inclination of the **E** vector to the (a,b) plane.

of the main peak towards low energy with increasing angle ($\Delta E = -215$ meV when Θ varies from 0° to 75°). This energy shift is still a puzzling result of XAS experiments, and up to now, its connection with the superconducting behavior is an open question. This shift is rather small in $La_{2-x}Sr_xCuO_4$ systems,[40,41] while it may amount from zero to a few hundreds of meV in BiSrCaCuO systems.[42] It is also obvious in Tl compounds,[39] but the authors do not comment on this experimental result.

Different interpretations can be developed:

(1) From Ref. 43, this energy shift is correlated with the T_c's and decreases when T_c increases for a given class of compounds.

(2) It has been argued[40] that this shift is a surface effect which is evidenced by the detection mode: total electron yield versus fluorescence yield.

(3) Recent angle-resolved photoemission experiments evidenced two CuO_2 bands crossing the Fermi level[44] which could be correlated to this result.

(4) This shift, finally, is a key ingredient of band-structure calculations[45,46] as well as a nonzero amount of z components of the doping holes.

In summary, there is to date no definite answer concerning this energy shift: Is it an experimental artifact or a real physical quantity? Does this shift rely on the class of compound and/or on the critical temperature, or does it just depend on the sample preparation and conditioning? Therefore, awaiting a more extended set of data, it seems worthwhile to point it out.

C. The superconducting ceramics

1. The basic ceramics

The copper L_3 edges of some thallium barium cuprates sinters, the Tl bilayer compounds Tl(2:2:0:1), Tl(2:2:1:2), and Tl(2:2:2:3) and a single-layer one Tl(1:2:2:3), have been also recorded and the doping hole densities deduced from the fit of the curve with two Lorentzians. One must be careful in comparing the doping hole densities n_h for various compounds, since absolute values of n_h may be affected by surface effects in the TEY mode of detection. However, good agreement exists between the estimated hole densities measured on the Tl(2:2:1:2) thin film and

the corresponding sinter ($n_h = 0.16$), both compounds exhibiting the same T_c. This result shows, at least for the same composition, the reproducibility of the XAS measurement.

2. *Annealings under soft reducing atmospheres*

To monitor the T_c's in thallium-layered cuprates, one can substitute thallium by divalent cations such as calcium and/or calcium by trivalent cations such as yttrium, lanthanum, and rare earths. In recent papers,[13,23] we have shown that, in solid solutions such as $TlBa_2Ca_{1-x}Y_xCu_2O_{7-\delta}$ $(0.2 \le x \le 1)$ and $Bi_{2-x}Pb_xSr_2Ca_{1-x}Y_xCu_2O_{8+\delta}$ $(0 \le x \le 1)$, the densities of doping holes in the $[CuO_2]_\infty$ planes decrease with increasing substitution rate x and vanish for $x > 0.6$. The decrease of the doping-hole densities can be correlated to the decrease of T_c's which vanish for $x > 0.5$. For both solid solutions, the optimum of T_c has been observed for a doping hole density of 0.14.

But, in such substituted systems, one cannot separate the real effect on the superconducting properties of the hole density variations from the one of the substitution of a divalent by a trivalent cation, like calcium by yttrium or a rare earth, which are close to the copper sites. To be definitely sure about the influence of the doping holes in the $[CuO_2]_\infty$ planes on T_c's, soft annealings at low temperature in a 10% H_2/Ar flux appear to be the best way to tune the doping hole density through small oxygen stoichiometry adjustments. Such annealings have been shown to induce a large increase of T_c in Tl(2:2:0:1) and rather a T_c optimization in Tl(2:2:1:2).[32,33]

We have used XAS at the copper L_3 edge to determine the variations of the doping hole densities in Tl(2:2:0:1) and Tl(2:2:1:2) ceramics as a function of annealing time.

a. Annealings of $Tl_2Ba_2CuO_6$. As published previously,[32,33] the ac magnetic-susceptibility curves of a Tl(2:2:0:1) ceramic (Fig. 6) show that the as synthesized pellet exhibits a T_c of 15 K and that the critical temperature increases drastically up to 87 K with increasing time of annealing. The corresponding x-ray absorption spectra at the Cu L_3 edge, recorded on the same samples as the ones characterized by ac susceptibility, have been plotted in Fig. 7 and compared to the Nd_2CuO_4 spectrum. A decrease of the $|3d^9\underline{L}\rangle$ peak intensity with the increasing annealing time can be observed and corresponds to the decrease of the doping hole density $n_h = I_{|3d^9\underline{L}\rangle}/(I_{|3d^9\rangle} + I_{|3d^9\underline{L}\rangle})$ deduced from the simulations (Table III). These results show that the large increase of T_c's in the Tl(2:2:0:1) cuprate originates in an optimization of the doping hole density in the $[CuO_2]_\infty$ planes.

b. Annealings of $Tl_2Ba_2CaCu_2O_8$. The way the superconducting properties of a Tl(2:2:1:2) pellet change after annealing under an H_2/Ar stream is close to the Tl(2:2:0:1) one.[32,33] The T_c's first increase from 107 to 115 K then stay constant, at least within the experimental errors, as well as the diamagnetic volumes for longer times of annealings as shown by ac susceptibility curves (Fig. 8). A post annealing under an O_2 stream can increase again the T_c and restore the grain boundaries.

The copper L_3-edge spectra of the same Tl(2:2:1:2) samples, as synthesized and annealed for various times as the ones characterized by ac susceptibility measurements, are shown in Fig. 9. Like in the annealings of the Tl(2:2:0:1) samples, the intensity of the high-energy shoulder at 932.5 eV ($|3d^9\underline{L}\rangle$ peak) decreases with increasing annealing times and the corresponding density

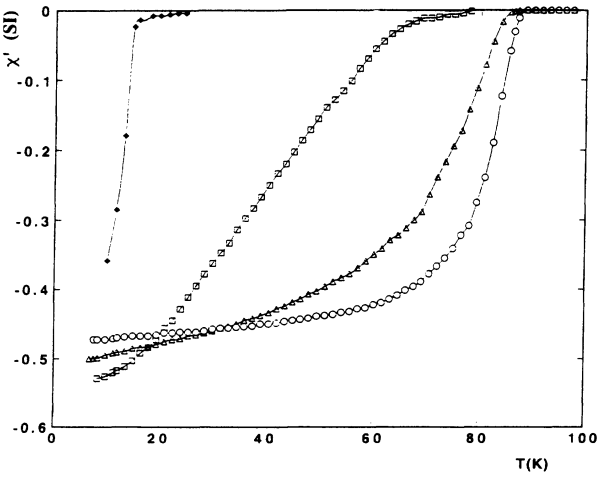

FIG. 6. ac susceptibility $\chi'(T)$ for annealed in 10% H_2/Ar samples of the $Tl_2Ba_2CuO_6$ type: as synthesized ♦, annealed during 20 min □, annealed during 40 min △, annealed during 60 min ○.

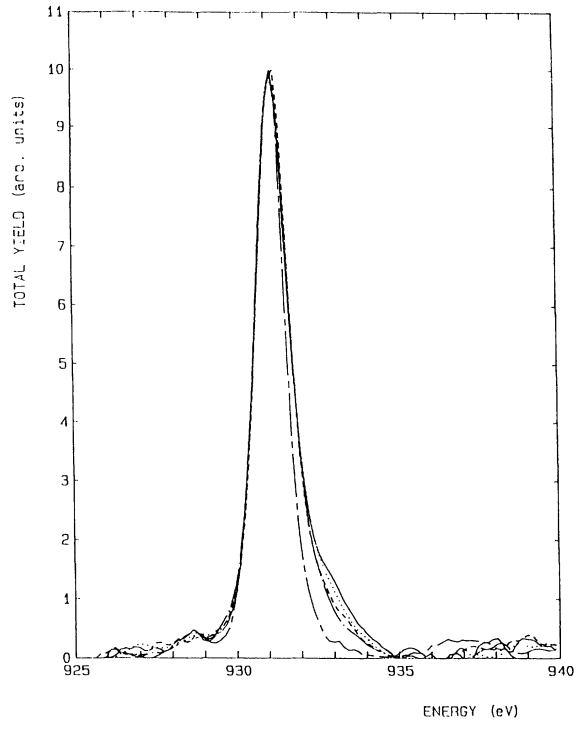

FIG. 7. Copper L_3 edge of Nd_2CuO_4 and the four annealed powder samples of the Tl(2:2:0:1) type: ------ Nd_2CuO_4, —— Tl(2:2:0:1) as synthesized, · · · · Tl(2:2:0:1) annealed during 20 min, - - - Tl(2:2:0:1) annealed during 40 min, —·—·— Tl(2:2:0:1) annealed during 60 min.

TABLE III. Simulation parameters of the copper L_3 edges for H_2/Ar annealed powder compounds of the Tl(2:2:0:1) and Tl(2:2:1:2) types. E and Γ are, respectively, the energy of the HWHM of the lines. $n_h = I_{|3d^9\underline{L}\rangle}/(I_{|3d^9\underline{L}\rangle} + I_{|3d^9\rangle})$ is the density of hole per copper.

Compounds annealing time		$\|3d^9\rangle$ $2p_{3/2} \rightarrow 3d^9$	$\|3d^9\underline{L}\rangle$ $2p_{3/2} \rightarrow 3d^9\underline{L}$	n_h (±0.015)	T_c (K) (±1)
2:2:0:1	E	931.1	932.45		
as synthesized	Γ	0.59	0.9	0.15	15
2:2:0:1	E	931.1	932.4		
20 min	Γ	0.60	0.9	0.135	66
2:2:0:1	E	931.1	932.5		
40 min	Γ	0.59	0.9	0.10	85
2:2:0:1	E	931.1	932.2		
60 min	Γ	0.61	0.9	0.09	87
2:2:1:2	E	931.1	932.54		
as synthesized	Γ	0.62	0.9	0.16	107
2:2:1:2	E	931.1	932.55		
10 min	Γ	0.63	0.9	0.13	111
2:2:1:2	E	931.1	932.40		
30 min	Γ	0.65	0.9	0.10	115
2:2:1:2	E	931.1	932.40		
40 min	Γ	0.60	0.9	0.08	112
	E	931.1	932.54		
2:2:2:3	Γ	0.63	0.9	0.17	125
	E	931.1	932.6		
1:2:2:3	Γ	0.7	0.9	0.17	115

of doping holes n_h decreases from 0.16, in fairly good agreement with the doping hole density recorded on the Tl(2:2:1:2) thin film, to 0.08 for the longest time of annealing (Table III).

Of course, all these calculated densities of holes cannot be considered as absolute values since the TEY detection may be influenced by surface effects although our results are close to those of the Fink's group recorded using EEL spectroscopy which is claimed to be a bulk spectroscopy. But what is important in this work is the relative variation of n_h with the annealing time and the reproducibility of the spectra on a large number of sample preparations.

Thus, these results show that small variations of the

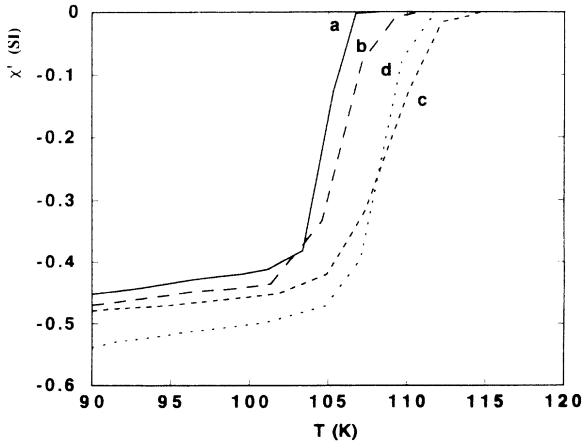

FIG. 8. Ac susceptibility $\chi'(T)$ for annealed in 10% H_2/Ar powder samples of the Tl(2:2:1:2) type: (a) as synthesized, (b) annealed during 10 min, (c) annealed during 30 min, (d) annealed during 40 min.

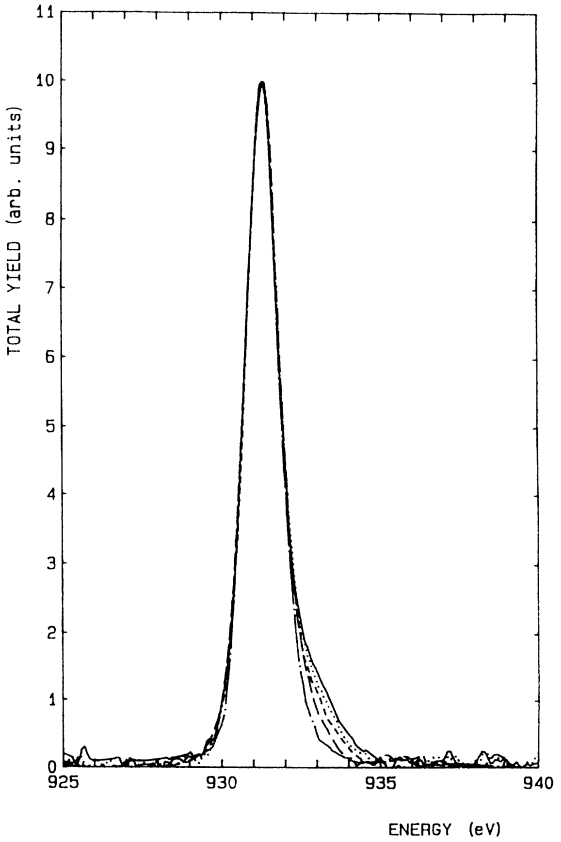

FIG. 9. Copper L_3 edge of Nd_2CuO_4 and the four annealed powder samples of the Tl(2:2:1:2) type: —·—·— Nd_2CuO_4, —— Tl(2:2:1:2) as synthesized, · · · · Tl(2:2:1:2) annealed during 10 min, --- Tl(2:2:1:2) annealed during 30 min, — — — Tl(2:2:1:2) annealed during 40 min.

doping hole densities can finely control the T_c's in the layered cuprates. Assuming that the doping hole densities change through small losses of oxygen during the annealing process, a 5% decrease of the doping hole densities corresponds to a loss of 0.025 and 0.05 oxygens for the Tl(2:2:0:1) and the Tl(2:2:1:2), respectively, losses not detectable by TGA analysis. The variations of T_c's as a function of the doping hole densities for all the thallium cuprates, studied by XAS in this work or in previous one,[13] are shown in Fig. 10; the existence of an optimum density of holes in the $[CuO_2]_\infty$ layers for the best T_c's is clearly evidenced.

It is also worth noting that, for the same variation of the doping hole density determined by XAS, the T_c increase appears large and drastic in Tl(2:2:0:1) whereas the T_c variations in Tl(2:2:1:2) are smaller and exhibit a smooth maximum. One can add that the Tl(2:2:2:3) compound shows no significant change in T_c under the same annealing treatment. Moreover, the T_c for the optimized Tl(2:2:0:1) ceramic (87 K), is quite different from the T_c's of the bilayer and three-layer compounds which are close (115 and 125 K, respectively). Hence it appears that the number of copper layers may also influence the superconducting properties in the thallium-layered cuprates. Here one can wonder about the origin of the oxygen atoms removed from the samples during the H_2/Ar annealing. From an oxygen K-edge analysis, Krol *et al.*[47] suggested recently that the oxygen losses, realized on a Tl(2:2:2:3) sinter after annealing under H_2 at low temperature (250 °C), might occur in the $[CuO_2]_\infty$ layers but this assumption is controversial with respect to the stability of these $[CuO_2]_\infty$ layers and to the neutron-diffraction experiments[48,49] which show that the oxygen vacancies are rather found in the $[TlO]_\infty$ layers. On the other hand, in thallium- and bismuth-bilayered cuprates, it is now well established that an electron transfer occurs from $[CuO_2]_\infty$ to $[Tl(Bi)O]_\infty$ layers which yields, at least, some amount of the hole density. The removal of some oxygen atoms in the $[Tl(Bi)O]_\infty$ layers will decrease the electron transfer and the doping hole density. Thus the variations of the doping hole density will also depend on the ratio of the number of $[CuO_2]_\infty$ over the number of $[Tl(Bi)O]_\infty$ layers. In this way, one can understand that the oxygen removal from the $[Tl(Bi)O]_\infty$ layers must more affect the single layer of the Tl(2:2:0:1), much less the double layer of the Tl(2:2:1:2) and affect very little the three layers of the Tl(2:2:2:3) in which the central layer can play the role of hole reservoir.

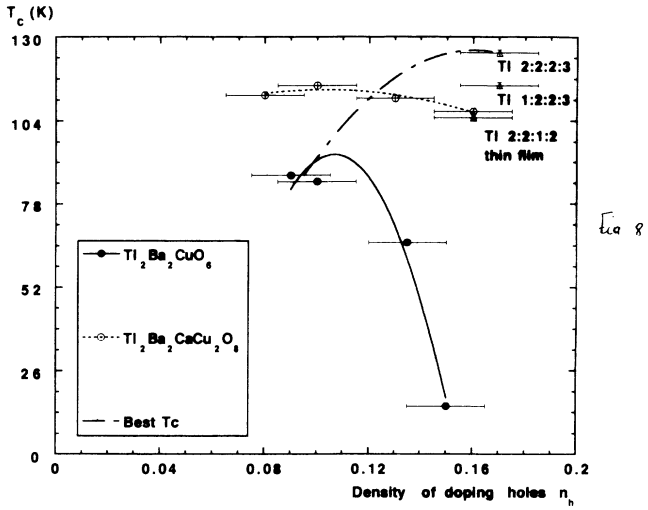

FIG. 10. The variations of T_c's versus the doping hole densities as determined by XAS in thallium cuprates. The curves correspond to the best fits for a set of points and are only given to guide the eye: —— Tl(2:2:0:1), · · · · Tl(2:2:1:2), ---- best T_c's in Tl(2:2:0:1), Tl(2:2:1:2), and Tl(2:2:2:3).

IV. CONCLUSION

This work has presented a study of the hole symmetries and densities in thallium-layered cuprates by XAS at the copper L_3 edge. The polarized spectra obtained on a Tl(2:2:1:2) thin film ($T_c = 105$ K) confirm the existence of a small density of covalent holes along the z axis in the copper $|3d_{z^2}^9\rangle$ orbital ($\approx 12\%$ of the density in the x,y plane) and the existence of doping holes only in the $[CuO_2]_\infty$ planes, the density of which being found to be 0.16 per copper in agreement with previous works on single crystals using EELS or fluorescence yield detection. Anyway this density of doping holes might not correspond to the optimum density since the highest T_c for this compound has been shown to be 115 K.

Annealing a Tl(2:2:0:1) ceramic under a 10% H_2/Ar stream allowed a decrease of the density of doping holes to be observed when the T_c's increase drastically, from 15 to 86 K, as shown by ac magnetic susceptibility. The same treatment, realized on a Tl(2:2:1:2) ceramic, led to a similar decrease of the doping hole density but with quite a smaller effect on T_c's which varied from 107 to 112 K through a maximum of 115 K. These results show that the density of holes must be optimized for the best T_c in thallium-layered cuprates such as in bismuth cuprates and that a too large hole density can reduce the T_c's drastically in a single $[CuO_2]_\infty$ layer compound but not in multilayers compounds.

ACKNOWLEDGMENT

The authors thank Professor B. Raveau for his support and fruitful discussions.

[1] A. Bianconi, A. Congiu Castellano, M. De Santis, P. Rudolf, P. Lagarde, A. M. Flank, and A. Marcelli, Solid State Commun. **63**, 1009 (1987).

[2] A. Bianconi, A. Congiu Castellano, M. De Santis, P. Delogu, A. Gargano, and R. Giorgi, Solid State Commun. **63**, 1135 (1987).

[3] D. E. Fowler *et al.*, Physica C **162-164**, 1303 (1989).

[4] D. K. Rai *et al.*, J. Appl. Phys. **66**, 3950 (1989).

[5]P. Steiner, S. Hüfner, A. Jungmann, V. Kinsinger, and I. Sander, Z. Phys. B **74**, 173 (1989).
[6]F. U. Hillebrecht *et al.*, Solid State Commun. **67**, 379 (1988).
[7]J. M. Imer *et al.*, Phys. Rev. Lett. **62**, 336 (1989).
[8]K. B. Garg *et al.*, Phys. Rev. B **38**, 244 (1988); K. V. R. Rao and K. B. Garg, Physica C **178**, 352 (1991).
[9]H. Tolentino *et al.*, Physica C **179**, 387 (1991).
[10]F. Studer *et al.*, Physica C **178**, 324 (1991).
[11]H. Tolentino, A. Fontaine, F. Baudelet, T. Gourieux, G. Krill, J. Y. Henry, and J. Rossat-Mignot, Physica C **192**, 115 (1992).
[12]A. Bianconi *et al.*, Physica C **153-155**, 115 (1988).
[13]N. Merrien, F. Studer, C. Martin, A. Maignan, C. Michel, B. Raveau, and A. M. Flank, J. Solid State Chem. **101**, 237 (1992).
[14]J. Fink *et al.* (unpublished).
[15]C. T. Chen *et al.*, Phys. Rev. Lett. **66**, 104 (1991).
[16]N. Nücker, J. Fink, J. C. Fuggle, P. J. Durham, and W. M. Temmerman, Phys. Rev. B **37**, 5158 (1988).
[17]J. M. Imer, F. Patthey, B. Bardel, W. D. Schneider, Y. Baer, Y. Petroff, and A. Zettl, Phys. Rev. Lett. **62**, 336 (1989).
[18]T. Takahashi *et al.*, Nature (London) **334**, 691 (1988); D. Van Der Marel, J. Van Elp, G. A. Savatzky, and D. Heitmann, Phys. Rev. B **37**, 5136 (1988).
[19]C. G. Olson *et al.*, Phys. Rev. B **42**, 381 (1990).
[20]Z. X. Shen *et al.*, Phys. Rev. B **39**, 823 (1989).
[21]B. O. Wells *et al.*, Phys. Rev. Lett. **65**, 3056 (1990).
[22]T. Watanabe *et al.*, Physica C **176**, 274 (1991).
[23]N. Merrien, F. Studer, G. Poullain, C. Michel, A. M. Flank, P. Lagarde, and A. Fontaine, J. Solid State Chem. **105**, 112 (1993).
[24]K. B. Garg, N. L. Saini, N. Merrien, F. Studer, S. Durcok, and G. Tourillon, Solid State Commun. **85**, 447 (1993).
[25]A. Bianconi, S. Dellalonga, C. Li, M. Pompa, A. Congiu Castellano, D. Udron, A. M. Flank, and P. Lagarde, Phys. Rev. B **44**, 10 126 (1991).
[26]M. Abbate, M. Sacchi, J. J. Wruk, L. W. M. Schreurs, Y. S. Wang, R. Lof, and J. C. Fugle, Phys. Rev. B **42**, 7914 (1990).
[27]N. Nücker, H. Romberg, X. X. Xi, J. Fink, B. Gegenheimer, and Z. X. Zhao, Phys. Rev. B **39**, 6619 (1989).
[28]E. Pellegrin, N. Nücker, J. Fink, S. L. Molodtsov, A. Gutiérrez, E. Navas, O. Strebel, Z. Hu, M. Domke, G. Kaindl, S. Uchida, Y. Nakamura, J. Markl, M. Klauda, G. Saemann-Ischenko, A. Krol, J. L. Peng, Z. Y. Li, and R. L. Greene, Phys. Rev. B **47**, 3354 (1993).
[29]H. Romberg, N. Nücker, M. Alexander, J. Fink, D. Hahn, T. Zetterer, H. H. Otto, and K. F. Renk, Phys. Rev. B **41**, 2609 (1990).
[30]J. P. Attfield and G. Ferey, J. Solid State Chem. **80**, 112 (1989).
[31]M. Hervieu, A. Maignan, C. Martin, C. Michel, J. Provost, and B. Raveau, J. Solid State Chem. **75**, 212 (1988).
[32]A. Maignan, C. Michel, M. Hervieu, C. Martin, D. Groult, and B. Raveau, Mod. Phys. Lett. B **2**, 681 (1988).
[33]M. Hervieu, C. Michel, A. Maignan, C. Martin, and B. Raveau, J. Solid State Chem. **74**, 428 (1988).
[34]A. Maignan, C. Martin, M. Huve, J. Provost, M. Hervieu, C. Michel, and B. Raveau, Physica C **170**, 350 (1990).
[35]C. Martin, A. Maignan, J. Provost, C. Michel, M. Hervieu, R. Tournier, and B. Raveau, Physica C **168**, 8 (1990).
[36]M. O. Krause and J. H. Oliver, J. Phys. Chem. Ref. Data **8**, 2 (1979).
[37]G. Demazeau, C. Parent, M. Pouchard, and P. Hagenmuller, Mater. Res. Bull. **7**, 913 (1972).
[38]W. Weber, Z. Phys. B **70**, 323 (1988).
[39]E. Pellegrin, N. Nücker, J. Fink, C. T. Simmons, G. Kaindl, J. Bernhard, K. F. Renk, G. Kumm, and K. Winzer, Phys. Rev. B **48**, 10 520 (1993).
[40]C. T. Chen, L. H. Tjeng, J. Kwo, H. L. Kao, P. Rudolf, F. Sette, and R. M. Fleming, Phys. Rev. Lett. **68**, 2543 (1992).
[41]E. Pellegin, N. Nücker, J. Fink, S. L. Molodtsov, A. Gutierrez, E. Navas, O. Strobel, Z. Hu, M. Domke, G. Kaindl, S. Uchida, Y. Nakamura, J. Markl, M. Klauda, G. Seamann, A. Krol, J. L. Peng, Z. Y. Li, and R. L. Greene, Phys. Rev. B **47**, 3354 (1993).
[42]A. Bianconi, C. Li, S. Della Longa, and M. Pompa, Phys. Rev. B **44**, 10 126 (1991).
[43]A. Bianconi, A. M. Flank, P. Lagarde, C. Li, L. Pettiti, M. Pompa, and D. Udron, *High-Temperature Superconductivity* (Plenum, New York, 1991), p. 363.
[44]D. S. Dessau, Z. X. Shen, D. M. King, D. S. Marshall, L. W. Lombardo, P. H. Dickinson, A. G. Loeser, J. DiCarlo, C. H. Park, A. Kapitulnik, and W. E. Spicer, Phys. Rev. Lett. **71**, 2781 (1993).
[45]C. Castellani, C. Di Castro, and M. Grilli, Physica C **153-155**, 1659 (1988).
[46]J. B. Grant and A. K. MacMahan, Phys. Rev. B **46**, 8440 (1992).
[47]A. Krol, C. S. Lin, Y. L. Soo, Z. H. Ming, Y. H. Kao, J. H. Wang, Min Qi, and C. S. Smith, Phys. Rev. B **45**, 10 051 (1992).
[48]B. Morosin, D. S. Ginley, E. L. Venturini, R. J. Baughman, and C. P. Tigges, Physica C **172**, 413 (1991).
[49]D. M. Ogborne, M. T. Weller, and P. C. Lanchester, Physica C **200**, 207 (1992).
[50]M. Pompa, P. Castrucci, C. Li, D. Hudron, A-M. Flank, P. Lagarde, H. Katayama-Yoshida, S. Della Longa, and A. Bianconi, Physica C **184**, 102 (1991).